Supplementary Information (SI) for Nanoscale.
This journal is © The Royal Society of Chemistry 2026

Electronic Supporting Information

Nitro Functionalization and Nanoscale Confinement Enable Ether-Based Quasi-Solid Electrolytes with Stable Lithium Metal and High-Voltage Compatibility

Huiling Liu[a,b] ‡, Xingkai Jia[a,b] ‡, Yu Xia[a,b], Zhu Liu[b], Yinzhu Jiang*[a,b], Xuan Zhang*[a,b]

[a] School of Materials Science and Engineering, Zhejiang University, Hangzhou 310027, China

[b] ZJU-Hangzhou Global Scientific and Technological Innovation Center, Zhejiang University, Hangzhou 311215, China

*Corresponding authors: E-mail: yzjiang@zju.edu.cn; xuanzhangzju@zju.edu.cn

‡ These authors contributed equally to this work.

Experimental

Materials: Zirconium tetrachloride ($ZrCl_4$, 99.9%), 1,4-benzenedicarboxylic (H_2BDC, 98%), 2-nitro-1,4-benzenedicarboxylic acid (2-NO_2-H_2BDC 98%), and N-methyl-2pyrrolidone(NMP, 99.8%) were purchased from Shanghai Aladdin Biochemical Technology Co., Ltd. N, N-Dimethylformamide (DMF, 99.5%) Ethanol (99.7%) and Hydrochloric acid (HCl, 36.0~38.0%) were purchased from Sinopharm Chemical Reagent Co., Ltd. NCM811 was purchased from Shenzhen Kejing STAR Technology Company. 1,2-dimethoxyethane (DME), propylene carbonate (PC), Lithium bis(trifluoromethanesulfonyl)imide (LiTFSI), Super P and lithium sheets were purchased from Suzhou Duoduo Chemical Technology Co., Ltd. Poly (vinylidene fluoride) (PVDF, M_w~534000) was purchased from Sigma-Aldrich. Al foil and coin-cell cases (CR2032) were purchased from Kelude Materials Technology Co., Ltd.

Synthesis and Preparation:

Synthesis of MOFs: UiO-66 and UiO-66-NO_2 were synthesized via a solvothermal method. The synthesis procedure for UiO-66-NO_2 is described as follows. First, 4.32 mmol (1.008 g) of $ZrCl_4$ was ultrasonically dissolved in a mixed solvent consisting of 5 mL of DMF and 8 mL of HCl in a 250 mL screw-cap glass bottle. Subsequently, 6 mmol (1.293 g) of 2-nitroterephthalic acid and 80 mL of DMF were added, followed by ultrasonication until a clear solution was obtained. The sealed bottle was then placed in a convection oven and maintained at 80 ℃ for 12 h. The resulting powder was collected by centrifugation and washed three times with DMF, followed by soaking in fresh DMF for 48 h. The solvent was replaced every 12 h. The sample was then immersed in ethanol for 24 h, with ethanol refreshed every 12 h. Finally, the MOF powder was recovered by centrifugation, dried at 80 ℃, and further activated under vacuum at 180 °C overnight. The activated UiO-66-NO_2 powder was stored in an argon-filled glovebox prior to use. UiO-66 was synthesized using an identical procedure, except that 2-nitroterephthalic acid was replaced with an equimolar amount of terephthalic acid.

Preparation of MOF-Based QSSEs: The preparation of the MOF-based QSSEs was carried out entirely in an argon-filled glovebox. Lithium bis(trifluoromethanesulfonyl)imide (LiTFSI, 2.871 g) was dissolved in 10 mL of 1,2-dimethoxyethane (DME) or propylene carbonate (PC) to obtain ether-based and ester-based electrolytes, respectively. Activated 4 Å molecular sieves were added to the electrolyte solutions, which were allowed to stand for at least 12 h to remove residual moisture,

yielding D-LE and P-LE electrolytes. Activated UiO-66 or UiO-66-NO_2 powders (60–90 mg) were then loaded into a stainless-steel die with an inner diameter of one-half inch and pelletized under pressures of 50, 100, or 150 MPa for 1 min. The resulting MOF pellets were immersed in D-LE or P-LE for more than 24 h to ensure complete electrolyte infiltration. After removal from the electrolyte, excess liquid on the surface was gently wiped off to obtain UP@D-LE, UNP@D-LE, or UNP@P-LE QSSEs.

Electrode preparation: The NCM811 cathode was fabricated through a blade-coating method. NCM811, Super P and poly (vinylidene fluoride) were mixed in a weight ratio of 8:1:1 in N-methyl-2-pyrrolidone. The slurry was spread onto a carbon-coated Al foil and heated at 100 ℃ under vacuum for 12 hours, and then cut into slices with a diameter of 10 mm. The areal mass loading of the NCM811 cathode was approximately 2.0 mg cm^{-2}, and the thickness of the Li foil was 177 μm.

Cell Assembly and Electrochemical Measurements

Ionic conductivity: Ionic conductivity was measured by electrochemical AC impedance spectroscopy (EIS) over a frequency range from 1 MHz to 0.1 Hz, with an AC amplitude of 10 mV, using a CHI760E electrochemical workstation. The variable temperature conductivity test was performed in a temperature-controlled chamber with test temperatures ranging from 30 to 90 ℃. The MOF-based quasi-solid-state electrolytes were sandwiched between two identical stainless steel (SS) blocking electrodes in 2025-type coin cells. Ionic conductivity (σ, S cm^{-1}) was calculated using the equation $\sigma = L / (R \times A)$, where R (Ω) is the ionic resistivity obtained from the Nyquist plot, L (cm) is the thickness of the electrolyte membrane, and A (cm^2) is the effective area of the SS electrode. The activation energy (E_a) was determined by fitting the temperature-dependent ionic conductivity data to the Arrhenius equation with a linear regression coefficient greater than 0.99.

Electrochemical stability window: The electrochemical stability window was determined by linear sweep voltammetry (LSV) using a stainless steel (SS)/electrolyte/Li cell configuration on a CHI760E electrochemical workstation. The voltage was scanned from open circuit potential to 6 V (vs. Li/Li^+) at a scan rate of 0.5 mV s^{-1}.

Lithium-ion transference number (t_{Li^+}): The lithium-ion transference number was determined using the amperometric method with an applied DC voltage of 10 mV, combined with electrochemical impedance spectroscopy (EIS) in a lithium symmetric cell containing the MOF-

based quasi-solid-state electrolytes. EIS measurements were performed before and after DC polarization, which was conducted via the amperometric technique. The t_{Li+} value was calculated according to Bruce's equation: $t_{Li+} = I_{SS}(\Delta V - I_0 R_0)/I_0(\Delta V - I_{SS} R_{SS})$ where ΔV is the polarization voltage (10 mV), I_0 is the initial current, I_{SS} is the stead-state current, R_0 is the initial resistance, and R_{SS} is the steady state total resistance.

Galvanostatic charge/discharge test: Lithium symmetric cells (Li/Li) and lithium half-cells (Li/NCM811) were assembled by sandwiching MOF-based QSSEs between two lithium metal discs or between a lithium metal disc and an NCM811 cathode slice, respectively. For lithium symmetric cells, galvanostatic tests were performed over a current density range from 0.1 to 11 mA cm^{-2}. Rate capability tests were conducted by cycling the cells for seven cycles at each current density. Critical current density (CCD) measurements were carried out using lithium symmetric cells with an initial current density of 0.1 mA cm^{-2}. The plating and stripping durations for each step were set to either 15 min or 60 min, and the current density was increased stepwise by 0.1 mA cm^{-2} or 0.4 mA cm^{-2}. Quasi-solid-state full cells were assembled in a Li||NCM811 configuration. Galvanostatic charge–discharge tests were conducted within voltage windows of 3.0–4.3 V or 3.0–4.4 V at current densities ranging from 0.1 C to 0.5 C, where 1 C corresponds to 207.9 mA g^{-1}. All electrochemical measurements were performed using CR2032-type coin cells.

Material characterization: Phase identification of the materials was carried out using an X-ray diffractometer (D2 PHASER, Bruker). The morphology and elemental composition were characterized by transmission electron microscopy and scanning transmission electron microscopy (Talos F200X S/TEM, Thermo Fisher Scientific). Specific surface areas and pore structures were analyzed using an automated surface area and porosity analyzer (ASAP 2460, Micromeritics, USA).

The chemical composition of the solid–electrolyte interphase was examined by X-ray photoelectron spectroscopy (K-Alpha, Thermo Fisher Scientific). Raman spectroscopy was performed using a laser Raman spectrometer (LabRAM HR Evolution, Horiba) to investigate the solvation structures of the electrolytes and MOF-based quasi-solid electrolytes. A 532 nm laser was selected according to the sample characteristics, and the Raman spectra were collected in the range of 500–1800 cm^{-1}. Thermogravimetric analysis was conducted using a thermal analyzer (STA 449 F5, NETZSCH) to

evaluate the thermal stability of the materials.

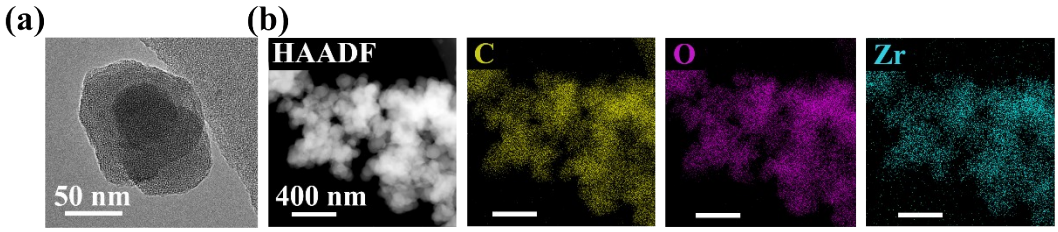

Fig. S1. (a) TEM images of UiO-66 powder and (b) the corresponding mapping results of C element, O element and Zr element at high-angle-annular-dark-field (HAADF) mode.

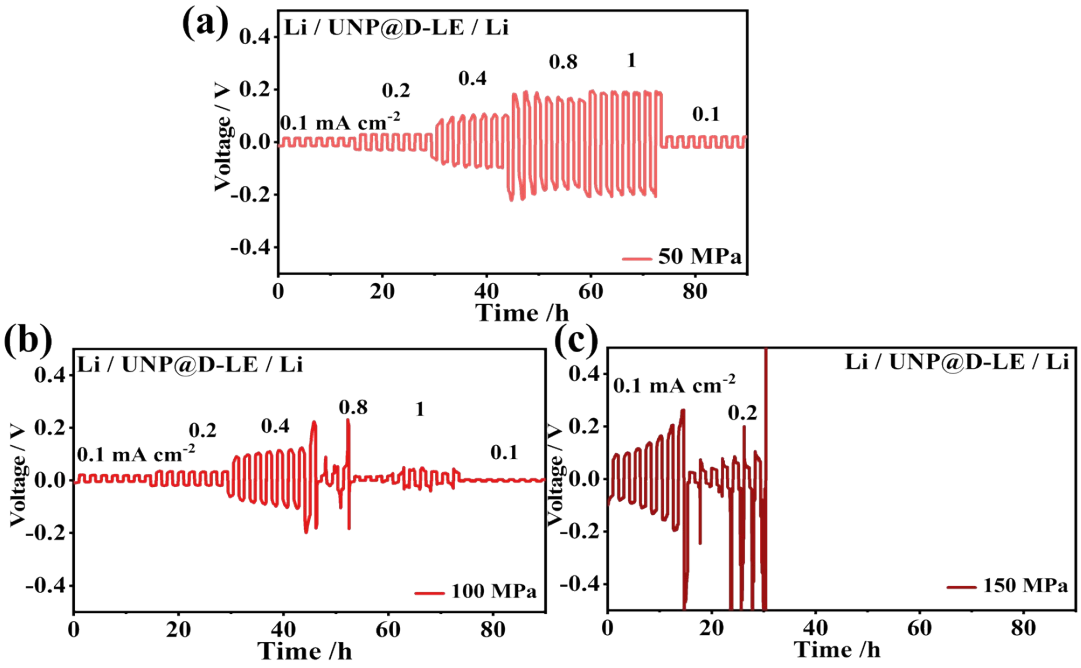

Fig. S2. Rate performance of Li symmetric cells with UNP@D-LE QSE prepared at (a) 50 MPa (b) 100 MPa and (c) 150 MPa.

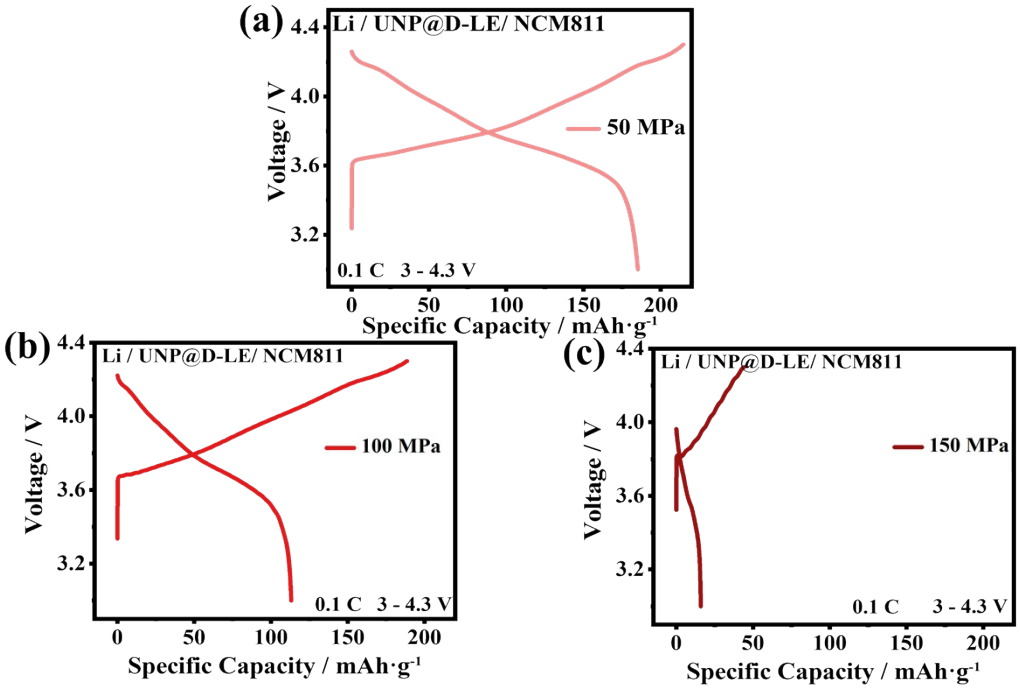

Fig. S3. Voltage-capacity curves (0.1 C, 3-4.3 V) of Li||NCM811 cells with UNP@D-LE QSE prepared at (a) 50 MPa (b) 100 MPa and (c) 150 MPa.

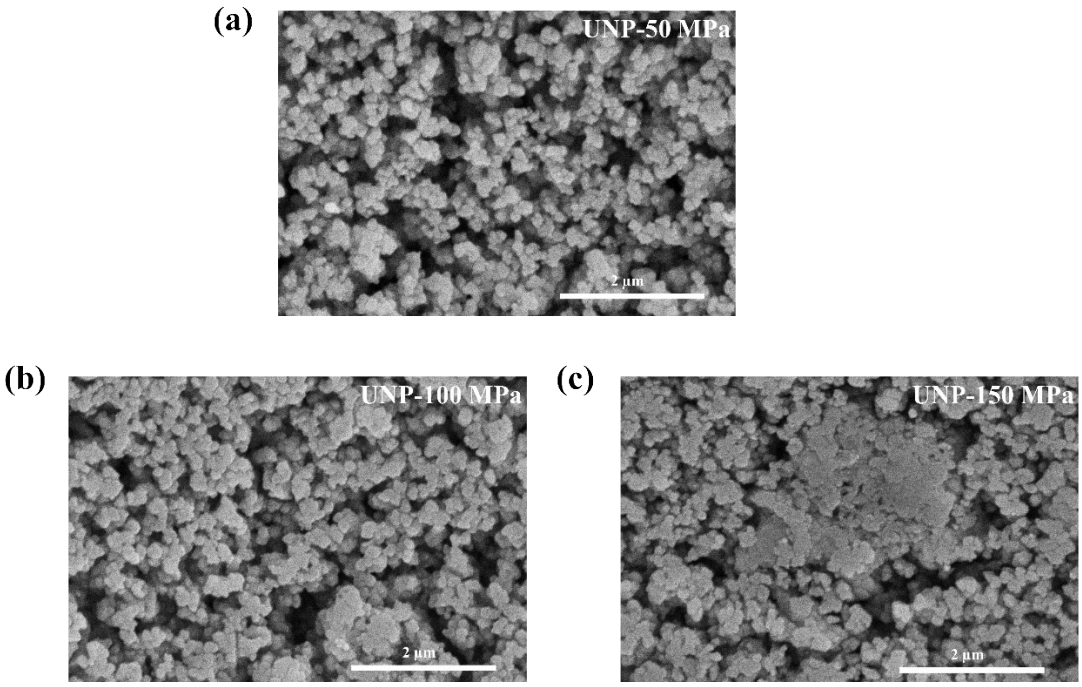

Fig. S4. Surface SEM images of UNP prepared under different pelletizing pressures: (a) 50 MPa, (b) 100 MPa, and (c) 150 MPa, showing the pressure-dependent variation in particle packing and pore structure.

(a)

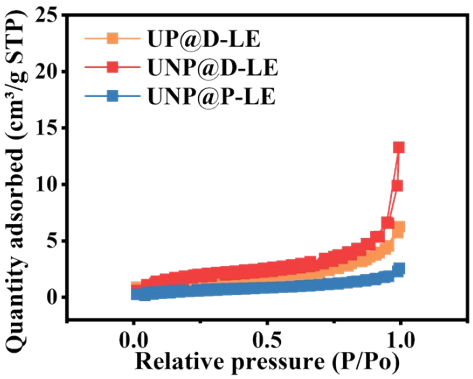

(b)

Sample	BET Surface (m^2/g)
UiO-66	1680
UiO-66-NO_2	823
UP@D-LE	5.29
UNP@D-LE	6.71
UNP@P-LE	2.41

Fig. S5. (a) N_2 adsorption/desorption isotherms of UP@D-LE, UNP@D-LE and UNP@P-LE. (b) Summary of BET surface area of UiO-66, UiO-66-NO_2, UP@D-LE, UNP@D-LE and UNP@P-LE.

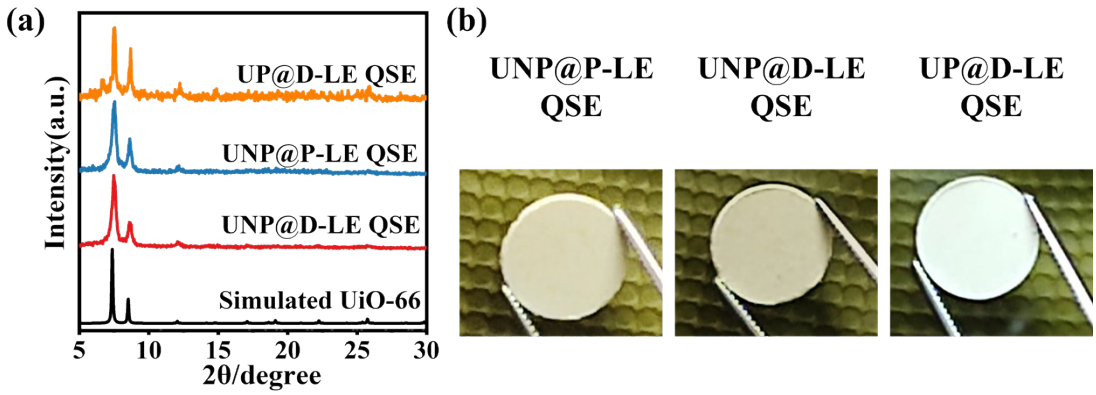

Fig. S6. (a) XRD patterns of UNP@D-LE, UNP@P-LE, UP@D-LE QSE and simulated UiO-66. (b) Optical images of UNP@P-LE (left), UNP@D-LE (middle) and UP@D-LE (right) QSE.

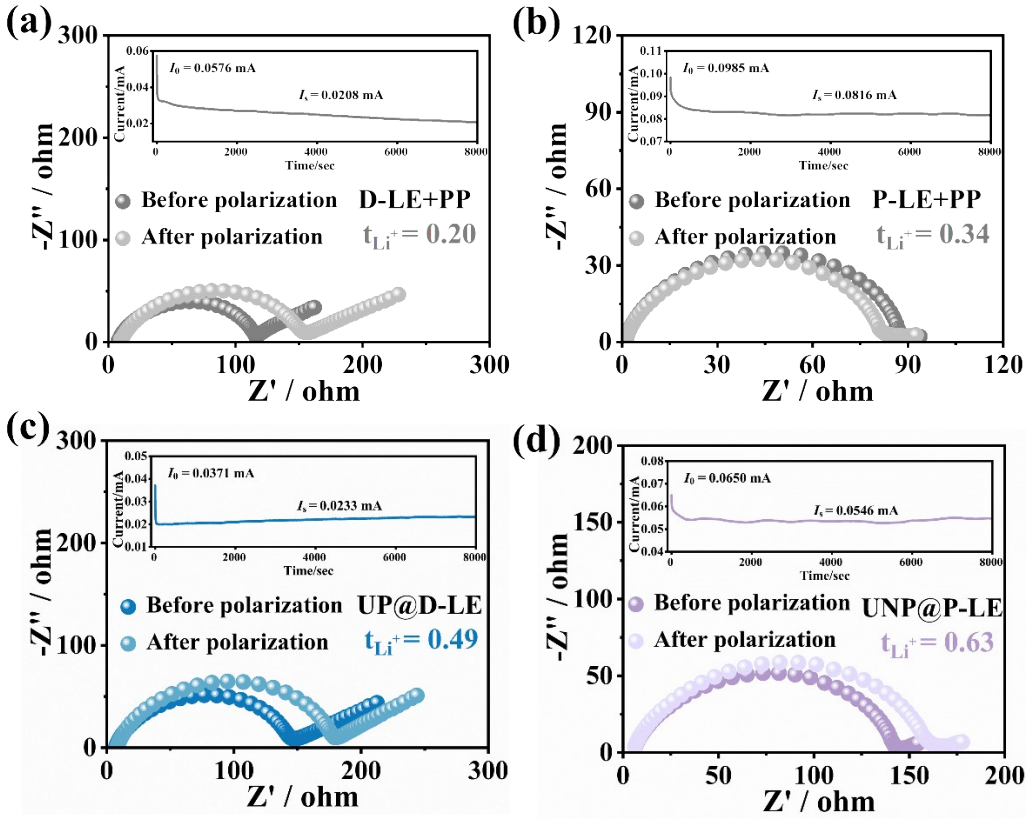

Fig. S7. Li ion transference number of (a) D-LE, (b)P-LE, (c)UP@D-LE and (d)UNP@P-LE.

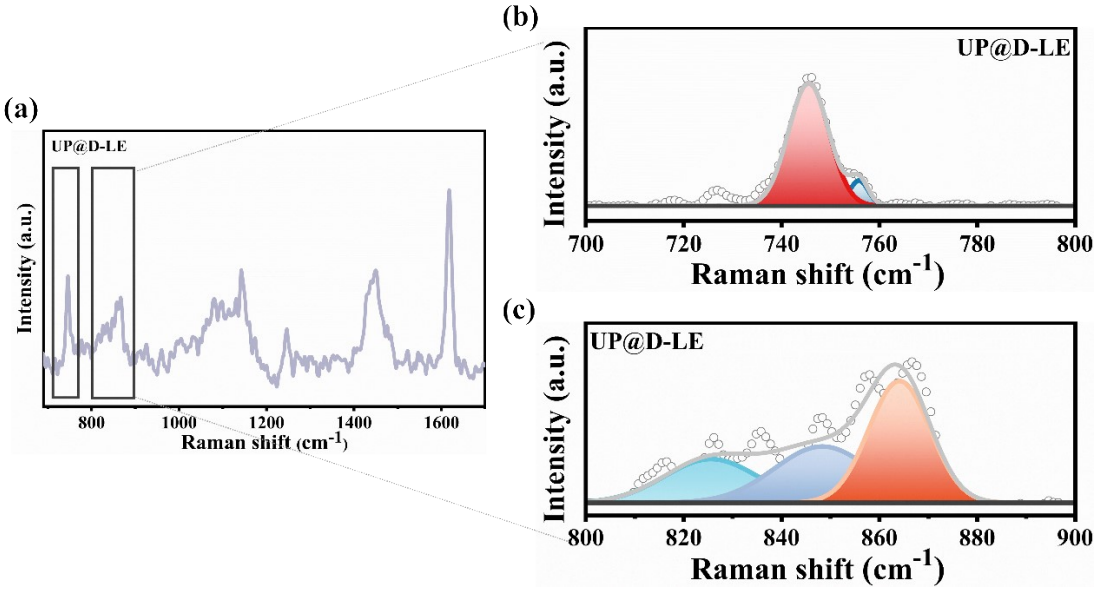

Fig. S8. Raman spectra of UP@D-LE.

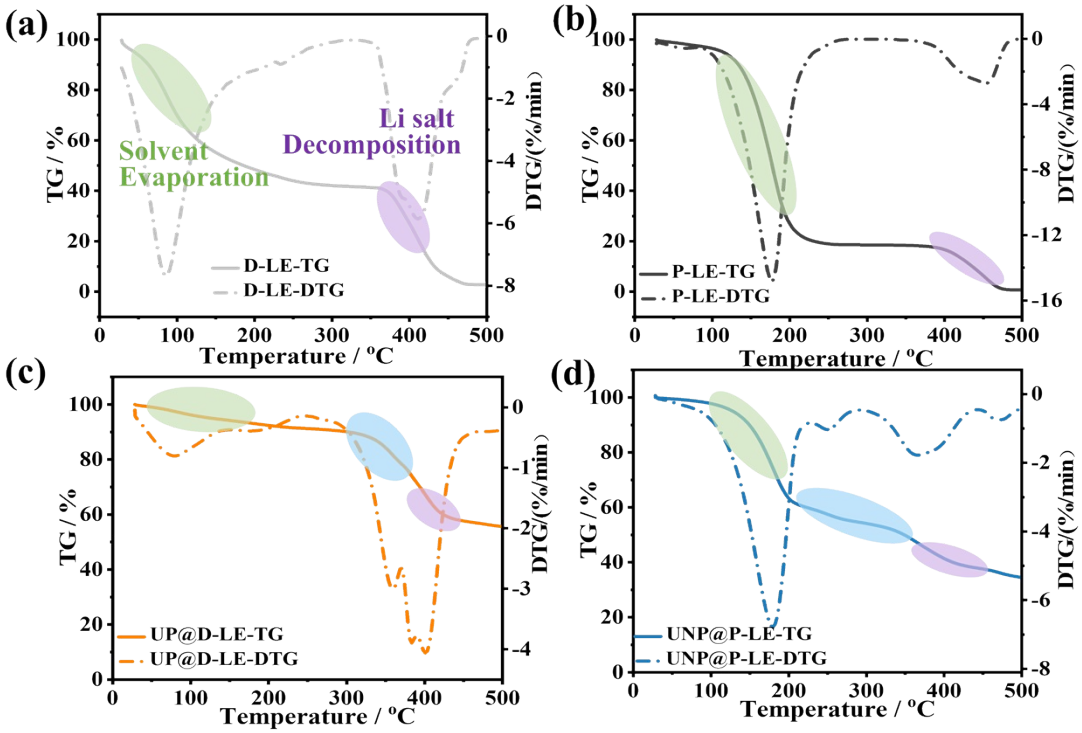

Fig. S9. Thermogravimetric analysis (TG) curves of (a) D-LE (1 M LiTFSI in DME), (b) P-LE (1 M LiTFSI in PC), (c) UP@D-LE, and (d) UNP@P-LE.

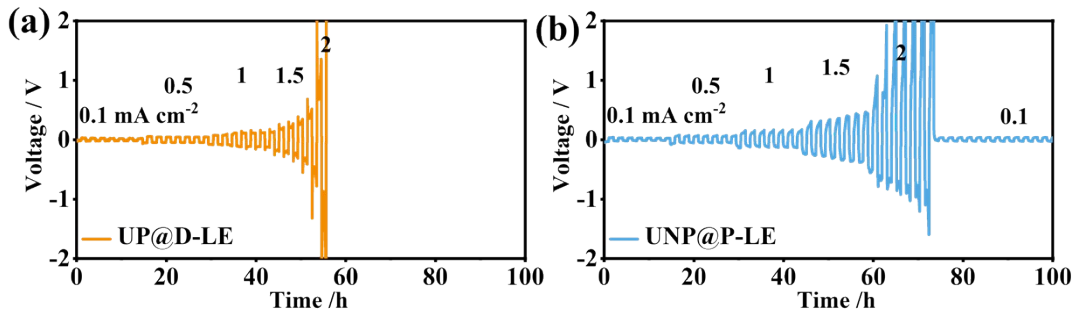

Fig. S10. Rate performance of lithium symmetric cells with (a) UP@D-LE QSE and (b) UNP@P-LE QSE.

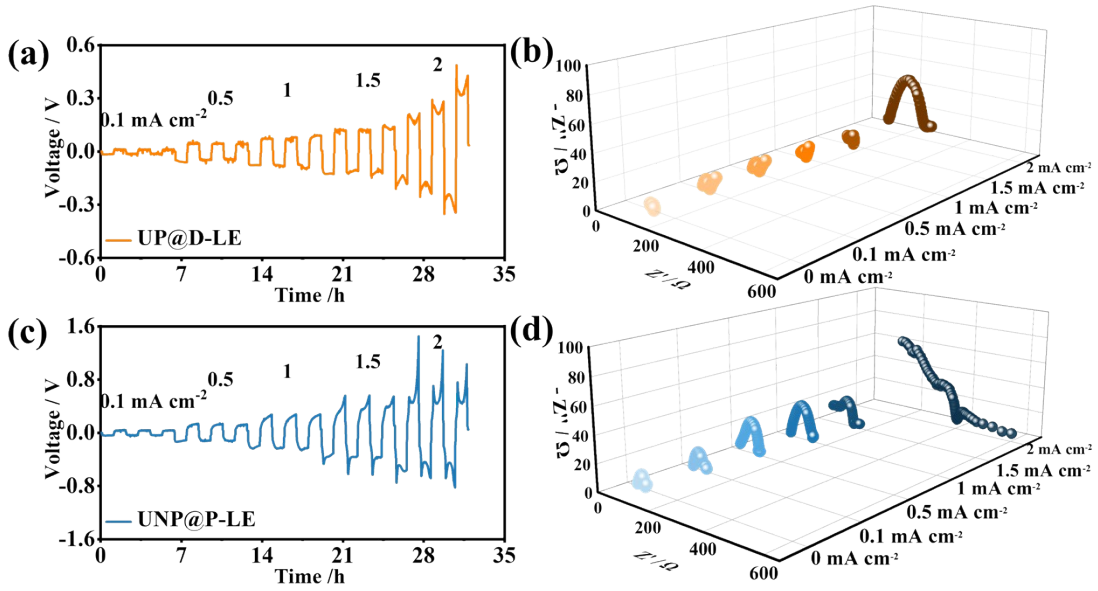

Fig. S11. Galvanostatic Li plating/stripping (left column) and EIS results (right column) of Li symmetric cells with UP@D-LE QSE (a-b) and UNP@P-LE QSE (c-d).

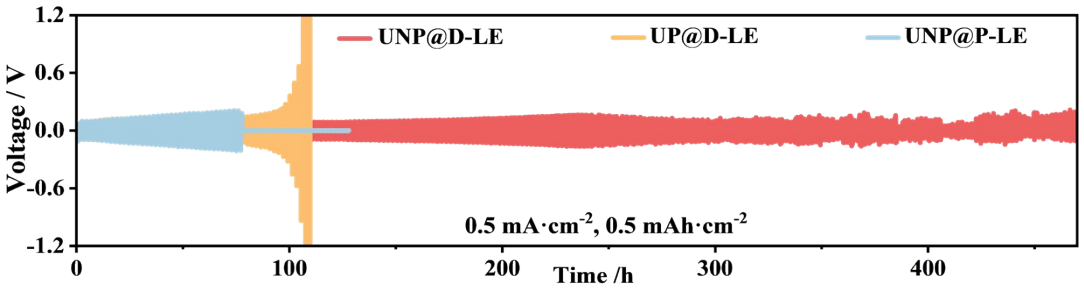

Fig. S12. Galvanostatic Li plating/stripping of symmetric cells with UP@D-LE, UNP@D-LE and UNP@P-LE QSEs at 0.5 mA cm^{-2}, 0.5 mAh cm^{-2}.

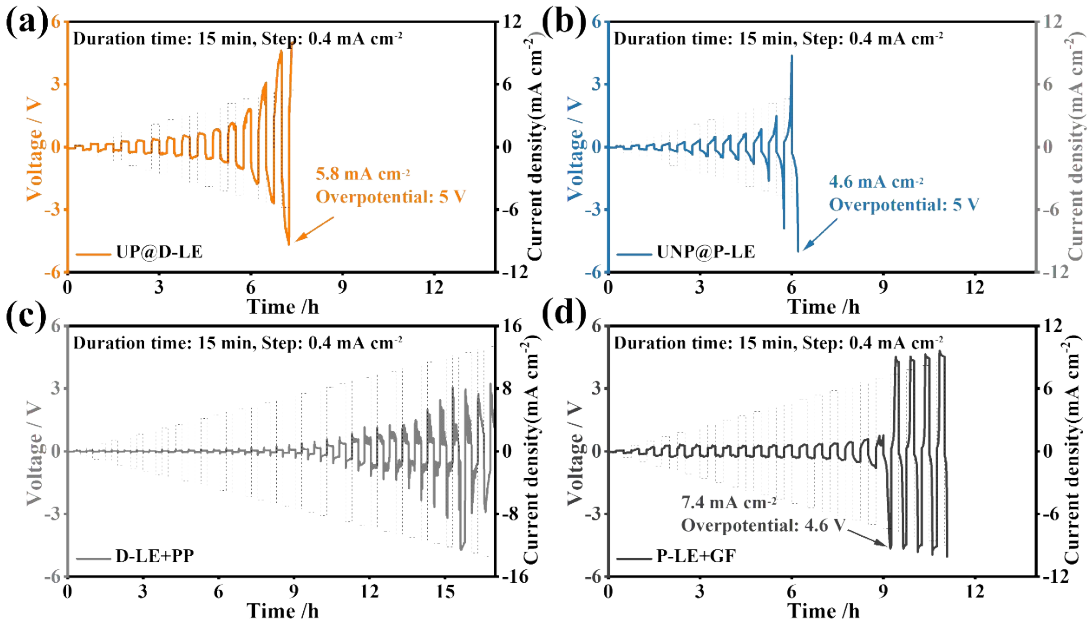

Fig. S13. CCD test with duration time of 15 min, start current density of 0.1 mA cm^{-2} and step size of 0.4 mA cm^{-2}: (a) UP@D-LE QSE, (b) UNP@P-LE QSE, (c) D-LE (1 M LiTFSI in DME) and (d) P-LE (1 M LiTFSI in PC).

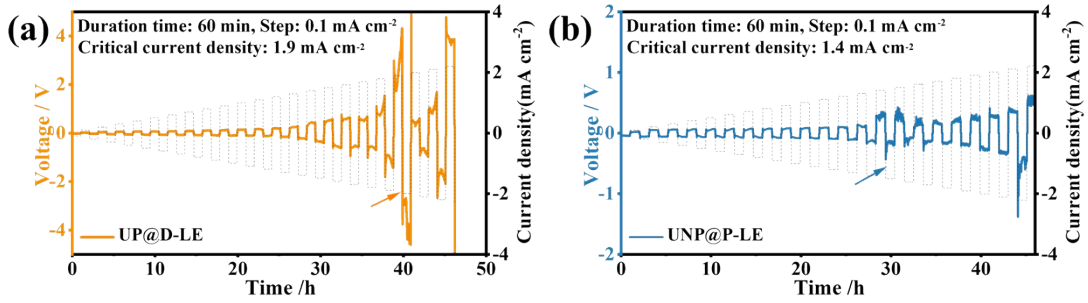

Fig. S14. CCD test with duration time of 60 min, start current density of 0.1 mA cm^{-2} and step size of 0.1 mA cm^{-2}: (a) UP@D-LE QSE and (b) UNP@P-LE QSE

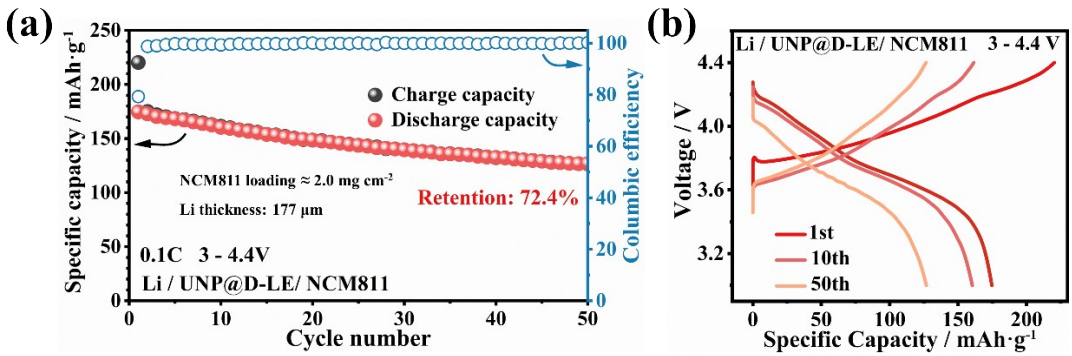

Fig. S15. (a) Cycling stability and (b) Voltage-capacity curves of Li||NCM811 cells with UNP@D-LE QSE at 0.1 C in the range of 3～4.4V.

Table S1. Reported CCD of MOF-based QSEs and test parameters

CCD (mA cm^{-2})	Initial current density (mA cm^{-2})	Step duration (min)	Current density step (mA cm^{-2})	Ref.
1	0.1	20	0.1	[1]
0.7	0.05	30	0.1	[2]
3	0.1	60	0.1	[3]
1.68	0.03	10	0.03	[4]
1.4	0.1	60	0.1	[5]
1.3	0.1	60	0.1	[6]
1.2	0.1	60	0.1	[7]

1 J.-H. Lee, H. Lee, J. Lee, T. W. Kang, J. H. Park, J.-H. Shin, H. Lee, D. Majhi, S. U. Lee, J.-H. Kim, *ACS Nano* **2023**, 17, 17372.

2 H. Jiang, Y. Du, X. Liu, J. Kong, M. Huang, P. Liu, T. Zhou, *J. Mater. Chem. A* **2023**, 11, 22371.

3 Z. Han, R. Zhang, J. Jiang, Z. Chen, Y. Ni, W. Xie, J. Xu, Z. Zhou, J. Chen, P. Cheng, *Journal of the American Chemical Society* **2023**, 145, 10149.

4 X.-L. Zhang, F.-Y. Shen, X. Long, S. Zheng, Z. Ruan, Y.-P. Cai, X.-J. Hong, Q. Zheng, *Energy Storage Mater.* **2022**, 52, 201.

5 W. He, D. Li, S. Guo, Y. Xiao, W. Gong, Q. Zeng, Y. Ouyang, X. Li, H. Deng, C. Tan, *Energy Storage Mater.* **2022**, 47, 271.

6 Q. Zeng, J. Wang, X. Li, Y. Ouyang, W. He, D. Li, S. Guo, Y. Xiao, H. Deng, W. Gong, *ACS Energy Lett.* **2021**, 6, 2434.

7 G. Wang, P. He, L. Z. Fan, *Adv. Funct. Mater.* **2021**, 31, 2007198.